Electromechanical Energy Conversion Systems (EECS)
Niroo Research Institute (NRI)
Vol. 3, No. 1, Autumn 2024, 36-42
DOI: 10.30503/eecs.2024.469349.1059
Original Article

Analysis of Induction Machine Drivers in Stationary Reference Frame with Time-Delay Model of Voltage Source Inverters

H. Sharifi[1], J. Nazarzadeh[1*]

Abstract

A precise current regulation in order to achieve accurate torque control is an important part of higher-performance control systems in vector-controlled induction motor drives. Applying the conventional controllers in the reference frame oriented to the rotor flux requires relatively complex hardware to measure the direct and quadrature components of the stator currents. On the other hand, using a suitable controller to adjust the stator current in the stationary frame is complicated due to the changes in the operation frequency of induction motors. In this paper, a frequency domain method for designing current controllers is introduced and applied to a vector-control of an induction motor in the stationary reference frame. This controller regulates currents of the induction motor with zero near steady-state error and a good transient performance while it is not sensitive to induction motor parameters. The performance of the controller is investigated with and without back electromotive force compensation signals. The validity of the introduced controller is confirmed by simulation and experimental results.

Keywords: Current Regulation, Vector-Controlled Drives, Induction Machines.

Received Date: 2024-07-23; Revised Date: 2024-10-10; Accepted Date: 2024-11-02.

Introduction

Designing of a current regulation is an important issue for virtually all high-performance electrical motor drive systems with dynamically accurate torque control. In order to achieve accurate torque control, modeling the machine in the conventional Rotor-Field-Oriented Reference Frame (RFORF) has been considered [1,2]. There are two strategies for controlling separately the torque and flux in Induction Motor (IM) drives. Direct Torque Control (DTC) [2, 3] adjusts the angle between stator and rotor flux vectors directly controlling the air gap torque and also consequently, keeps the magnitude of the stator flux vector constant [4]. Besides, a fast dynamic response, minimal torque response time, and inherent simplicity [2] can be considered as the major advantages of DTC. In addition, the variation of the switching frequency according to the amplitude of the hysteresis bands and the motor operating speed, non-optimized selection of voltage vectors, and high ripple torque are their disadvantages of DTC. Therefore, use of comparators with and without hysteresis, and implementation of DTC schemes for constant switching frequency operation with Pulse Width Modulation (PWM) or Space Vector Modulation (SVM) techniques have been proposed to overcome these problems [5]. The use of these methods increases the complexity of the control technique in DTC and decreases the simple control structure of DTC [6]. In addition, DTC requires a precise flux and torque estimator, and does not meet demand for low-speed operation [7].

Field-Oriented-Control (FOC) [8,9] decouples the torque and flux producing components of stator current vectors in order to achieve fast torque regulation. Tracking the recommended value of reference current in the RFORF is an important part of a precise current regulator for FOC [10]. As a result, FOC can operate smoothly over the wide speed range, produce full torque at zero speed, and control torque at low frequencies and speeds. Besides, the existence of nonlinear phenomena which degrades the performance of vector-controlled IM drives has been investigated in [11].

There are two common controllers for current regulation. Hysteresis controllers generate the switching states of a Voltage Source Inverter (VSI) by using instantaneous comparisons between required commended reference and measured currents. These controllers have the advantages of no complex implementation, fast dynamic response, insensitivity to load parameter variations, and direct over current protection [12,13]. The hysteresis controllers, however, have the disadvantage of a

1. Engineering Faculty, Shahed University
**Corresponding author, Email: nazarzadeh@shahed.ac.ir*

variable inverter switching frequency [13]. In addition, a Maximum Switching Frequency (MSF) can be very high and thus, affects the stable operation range of the controller. A proposed solution in [14] limited the MSF within the stable operation range. However, this has the disadvantage of making distortion in the inverters output current resulting in producing low order harmonic components as noises and losses. Linear current regulators generate the switching states by comparing a low frequency error current with a high frequency triangle wave and also minimize the current error.

A Proportional-Integral (PI) current regulator in the RFORF has been commonly used, due to its zero steady-state current error. Using a stable PI controller in simple converters such as buck or boost also requires complex hardware because the dynamic model of the system is bilinear [15]. This condition also exists in the two-axis model of the IM the RFORF. However, requiring two transformations between synchronous and the SRF, and decoupling circuits with the complexity of measurements and implementation are its drawbacks [16]. In addition, the PI current regulators in Stationary Reference Frame (SRF) are regarded as having inability to track precisely ac current references in IM drives. Also, a feed forward compensating signal is needed for achieving proper current regulation in SRF. This signal is back-EMF of the IM [9]. Next to it, when an IM operates in high-speed ranges, the induced back-EMF signals of the IM may exceed the limitation of the stator voltage [17]. Also, the PI controller has the disadvantage of complexity of implementation and computing the back-EMF signals in the RFORF.

On the other hand, a different type of the SRF current regulator called Proportional-Resonant (PR) has been considered [18] to reduce the steady-state error [9,19]. This regulator has two poles on imaginary axes considered as its disadvantage [20] in the SRF. On the other hand, the feeding frequency of an IM drive is varied proportional to the changing load conditions. Therefore, to use a PR controller in an IM drive, it is necessary to adjust the controller poles according to the supply frequency so that the PR controller is able to current track with zero error any operating conditions. This has a great limitation in using a PR controller in an IM drive system.

In this paper, a technique for designing the proposed current controller in the SRF is introduced with near zero steady-state error, a good transient performance and minor reliance on the speed measurement, because of eliminating the back-EMF feed forward correction signals. First of all, the model of the IM for decoupling control of the torque and flux is considered. Then, to investigate the sensitivity of the proposed controller performance to the variation of the machine parameters, the frequency responses of the controller are analyzed considering the uncertainty of the IM parameters. Also, the controller parameters are designed on proper values for achieving higher performance. In contrast to the conventional current regulator in the RFORF, the sensitivity of the proposed controller has completely decreased or eliminated machine parameter variations and back-EMF signals. Finally, the close-loop proposed regulator performances have been confirmed by some numerical and experimental results.

2. MODEL OF THE IMs FOR FOC

The space phasors of the IM voltage relations in the RFORF are

$$\vec{v}_s = R_s\vec{i}_s + p\vec{\psi}_s + j\omega_e\vec{\psi}_s \quad (1)$$

$$\vec{v}_r = R_r\vec{i}_r + p\vec{\psi}_r + j(\omega_e - \omega_r)\vec{\psi}_r = 0 \quad (2)$$

where R_s, R_r and p are the stator, rotor resistances and the d/dt operator, respectively. Besides, ω_e is the angular speed of the rotor flux phasor ($\vec{\psi}_r$) and and, ω_r is the electrical speed of the rotor. Also, subscripts "s" and "r" are the stator and rotor phasors of fluxes and voltages in the RFORF, respectively. Also, the rotor voltage phasor is considered zero. Moreover, the space phasors of stator and rotor currents are given in the RFORF as $\vec{\imath}_s = i_{sx} + ji_{sy}$ and $\vec{\imath}_r = i_{rx} + ji_{ry}$ respectively, where i_{sx}, i_{sy} and i_{rx}, i_{ry} are the direct- and quadrature-axis currents of the stator and rotor, respectively in the RFORF. Next, the rotor flux-linkage space phasor in this frame can be written as

$$\vec{\psi}_r = L_m\vec{i}_s + L_r\vec{i}_r \quad (3)$$

where L_m and L_r denote the magnetizing and rotor inductances, respectively. Since ψ_{ry}, the quadrature-axis component of the rotor flux-linkage in the RFORF, electromagnetic torque production of an IM (T_e) with P pole-pairs in terms of the two-axis components of the RFORF can be expressed as

$$T_e = \frac{3}{2}P\frac{L_m}{L_r}\psi_{rx}i_{sy} \quad (4)$$

in which ψ_{rx} is the direct-axis component of the rotor flux-linkage. Since ψ_{ry}=0 in the RFORF, the rotor quadrature-axis current can be expressed in terms of the stator quadrature-axis current as

$$i_{ry} = -\frac{L_m}{L_r}i_{sy} \quad (5)$$

with some manipulation, by substituting Eq. (5) into the imaginary-axis component of Eq. (2), the relation of the angular slip frequency can be written as

$$s\omega_e = \frac{1}{\tau_r}i_{sy}\frac{L_m}{\psi_{rx}} \quad (6)$$

where the rotor time constant is τ_r=L_r/R_r and s denote the motor slip defined as s=(ω_e-ω_r)/ω_e. Next, since ψ_{ry}=0 and ψ_{rx} is a constant, the real-axis

component of Eq. (2) can be rearranged to express as

$$i_{rx} = -\frac{p\psi_{rx}}{r_r} = 0 \tag{7}$$

The required mutual relationship ψ_{rx}, i_{rx} and also a required ψ^*_{rx}, i^*_{sx} (the reference value of i^*_{rx}) by substituting Eq. (7) into the imaginary-axis component of Eq. (2) can be expressed as

$$i_{sx} = \frac{\psi_{rx}}{L_m} \tag{8}$$

$$i^*_{sx} = \frac{\psi^*_{rx}}{L_m} \tag{9}$$

The vector-controlled principles for an IM can be considered as commending i^*_{sx} and i^*_{sy}. In simpler terms, i^*_{sx} sets ψ^*_{rx} to a certain value, and i^*_{sy} meets the required torque. Continuously determining the axis angle of the RFO, ρ_r is an important factor of a vector control. By integrating and adding the angular rotor speed and slip frequency together, the rotor-flux-axis angle can be calculated. A mechanical speed encoder is set on the motor shaft to measure the rotor angular speed and its position. In addition, the angular slip frequency can be achieved by using Eq. (9). The equation of constantly calculating ρ_r can be expressed as

$$\rho_r = \int \omega_r dt + \int s\omega_e dt = \theta_r + \frac{1}{\tau_r}\int i_{sy}\frac{L_m}{\psi_{rx}}dt \tag{10}$$

The commended values of i^*_{sx} and i^*_{sy} should be substituted rather than measured i_{sx} and i_{sy} respectively for simplifying in calculation the Eq. (10). This suggestion introduces a small residual error between the measured and commended values of i^*_{sx} and i^*_{sy} in transient period.

$$\rho_r \approx \theta_r + \frac{1}{\tau_r}\int \frac{i^*_{sy}}{i^*_{sx}}dt \tag{11}$$

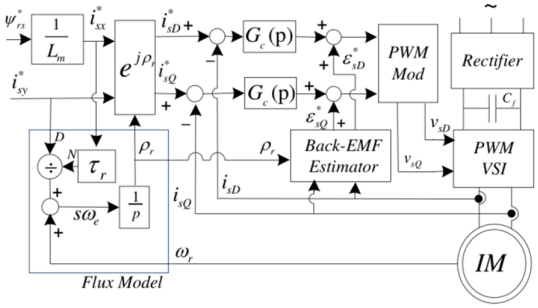

Fig.1. FOC with current regulator and decoupling in the SRF.

3. CURRENT REGULATOR IN THE SRF

The current controller in the SRF is a well-known classical regulator. It uses current errors to produce the voltage commands. Fig. 1 depicts these regulators for a FOC drive. With regard to back-EMF, the direct- and quadrature-axis of the IM stator voltages, v_{sD} and v_{sQ}, in the stationary reference frame can be expressed as

$$v_{sD} = R_s i_{sD} + pL'_s i_{sD} + e_{sD} \tag{12}$$

$$v_{sQ} = R_s i_{sQ} + pL'_s i_{sQ} + e_{sQ} \tag{13}$$

where $L'_s = L_s - (L^2_m/L_r)$. Also, the e_{sD} and e_{sQ} named the mutual coupling (back-EMF) signals can be obtained as [9]

$$e_{sD} = -\frac{L^2_m}{L_s L_r}\omega_e \psi_{sx} \sin\rho_r \tag{14}$$

$$e_{sQ} = +\frac{L^2_m}{L_s L_r}\omega_e \psi_{sx} \cos\rho_r \tag{15}$$

By generating and adding the mutual coupling terms to the voltages applied to the IM, the mutual coupling terms can be eliminated or decreased. Thus, the motor applied voltages can be expressed as

$$v_{sD} = v_{sDcon} + e^*_{sD} \tag{16}$$

$$v_{sQ} = v_{sQcon} + e^*_{sQ} \tag{17}$$

where v_{sDcon} and v_{sDcon} are the current controller outputs depicted in Fig. (2). And also, e^*_{sD} and e^*_{sQ} are back-EMF feed-forward correction signals which can be written as

$$e^*_{sD} = -\frac{1}{V_{DC}}\frac{L^2_m}{L_s L_r}\omega_e \psi_{sx} \sin\rho_r \tag{18}$$

$$e^*_{sQ} = +\frac{1}{V_{DC}}\frac{L^2_m}{L_s L_r}\omega_e \psi_{sx} \cos\rho_r \tag{19}$$

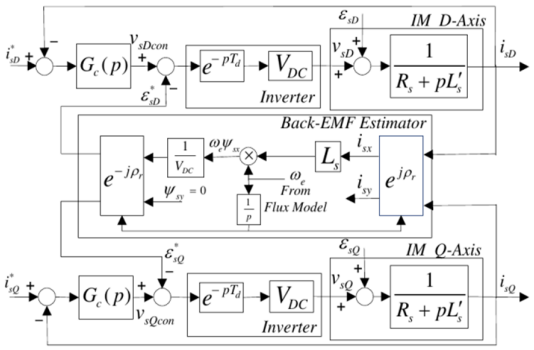

Fig.2. Block diagram of the proposed current regulator in the SRF.

where its DC bus voltage (V_{DC}) result in a dimensionless quantity as a gain. These signals are added to the PWM target commended voltages and then, the direct- and quadrature-axis of stator voltages in the SRF can be expressed as

$$v_{sDcon} = R_s i_{sD} + pL'_s i_{sD} \tag{20}$$

$$v_{sQcon} = R_s i_{sQ} + pL'_s i_{sQ} \tag{21}$$

4. DSSGINING CURRENT CONTROLLER IN THE SRF

A current controller with low offset, noise and drift effects can be expressed as

$$G_c(p) = k_p + \frac{k_i}{1+\tau_i p} \tag{22}$$

By concerning, in high frequency ranges, $\tau_i\omega >> 1$, dynamical performances of this current controller in Eq. (22) are significantly similar to a PI controller. In this paper, as examining the amplitude and phase response curves in details plays a key role in designing the controller parameters in vector control drives. Fig. (2) shows a stationary current regulator with back-EMF. In this figure, the PWM inverter is modeled by a time-delay (T_d) and a linear gain V_{DC}, respectively.

Dynamic model of the PWM modulator in Fig. (2) has a direct effect on the response of the closed-loop control system. If the control signal is sampled by an ideal A/D converter at twice the carrier frequency, the average time-delay between the output and input of the modulator will be half the period of the carrier signal. On the other hand, an A/D converter in the digital control system can increase the time-delay of the system. Also, by increasing the time-delay in the modulator and A/D converter, the stability margin of the system is reduced. Therefore, the model of a modulator with an A/D converter can be considered with a time-delay of T_d=0.75 T_s in the worst case [18]. Hence, the open loop transfer function of the system is

$$G(p) = \frac{k_p(1+\tau_i p)+k_i}{(1+\tau_i p)(R_s + pL_s')} e^{-pT_d} V_{DC} \tag{23}$$

For this above-mentioned purpose, tendency to maximize the proportional gain k_p and current loop integration gain k_i is taken into consideration. In the meanwhile, the effect of time-delay (e^{-pTd}), and a target phase margin (φ_m) are taken into account as well. The cross over frequency (ω_c) is given by

$$\angle G(j\omega_c) = -\pi + \varphi_m \tag{24}$$

That is a given that as mentioned above the fact that $|\tau_i\omega_c| >> 1$, $\tan^{-1}(\tau_i\omega_c)$ can be somewhere in the vicinity of $\pi/2$. Hence, using Eqs. (23) and (24), we have

$$\varphi_m \approx \pi - \omega_c T_d - \tan^{-1}(\tau_s'\omega_c) - \tan^{-1}\left(\frac{k_p\tau_i\omega_c}{k_p+k_i}\right) \tag{25}$$

where $\tau'_s = L'_s/R_s$ is transient time constant of an IM. Also, if the value of $\tan^{-1}(k_p\tau_i\omega_c/(k_i+k_p))$ is assumed $\pi/4$ thus, Eq. (25) can be rewritten as

$$\omega_c \approx \frac{1}{\tau_s'}\tan\left(\frac{3\pi}{4} - \varphi_m - \omega_c T_d\right) \tag{26}$$

This relation can be solved for ω_c by iterative method for given τ'_s, φ_m and T_d. By assuming $\tau_i\omega_c >> 1$, τ_i can be expressed as

$$\tau_i = \frac{100}{\omega_c} \tag{27}$$

concerning $\tan^{-1}(k_p\tau_i\omega_c/(k_i+k_p)) = \pi/4$ and with regard to $|\tau_i\omega_c| >> 1$, k_i in the term of k_p can be written as

$$k_i = k_p(\tau_i\omega_c - 1) \approx k_p\tau_i\omega_c \tag{28}$$

from Eqs. (23) and (28) and by setting the open loop gain equal to unite value ($|G(j\omega_c)|=1$) with concerning ($\omega_c\tau'_s$) >> 1, we have

$$k_p = \frac{R_s}{\sqrt{2}V_{DC}}\sqrt{1+(\tau_s'\omega_c)^2} \approx \frac{\omega_c L_s'}{\sqrt{2}V_{DC}} \tag{29}$$

TABLE. 1. Vector-controlled drives

Parameter	values
Induction Motor (4P)	175 w, 220 v, 0.75 A
R_s	43.16 Ω
R_r	75 Ω
L_s	1.995 H
L_r	1.995 H
L_m	1.96 H
Maximum Sample Frequency	1 kHz
V_{DC}	160 V
φ_m	0.175 rad
ω_c	1.38 krad/sec
k_p	0.42
k_i	41.86
τ_i	72.5 msec

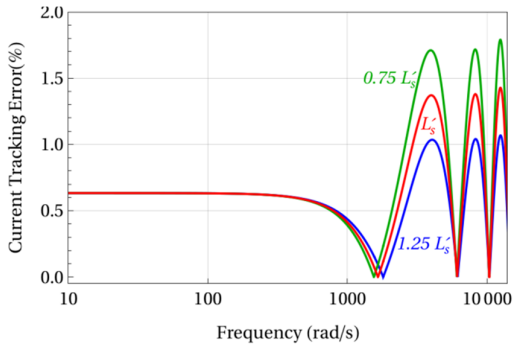

Fig.3 Frequency response of the proposed current regulator in the SRF for tracking error in percentage with different transient inductances.

Using Eqs. (26) to (31), we are able to design parameters of the current controllers for FOC drives in the SRF. Table 1 shows typical parameters of the proposed controller for an IM. For $\varphi_m=\pi/18$, using Eq. (26) we get ω_c=1.37 krad/sec. Moreover, from Eq. (31) we can obtain k_p=0.42 and by applying results in Eqs. (27) and (29), τ_i and k_i are determined 72.5 msec and 41.86, respectively.

5. THE FREQUENCY ANALYSIS OF THE CURRENT CONTROLLER

Regarding Fig. (2), the closed-loop and back-EMF transfer function are clearly defined as $G_i(p)=i_{sD}/i^*_{sD}$ and $G_e(p)=i_{sD}/\varepsilon_{sD}$, and then the effect of the IM parameter L_s' on the $G_i(p)$ and $G_e(p)$ frequency response is shown in Figs. (3) and (4), receptively. The parameters used in this analysis are introduced in Table 1. By considering $i_{sD}=G_i(p)i^*_{sD}+G_e(p)\varepsilon_{sD}$ in the current control system, it is the most important desires to reach a reasonable compromise between $|G_i(j\omega_c)|\approx1$ and $|G_e(j\omega_c)|\approx0$. Fig. (3) shows the frequency responses of the proposed controller for tracking error $(|1-G_i(j\omega))$ in percentage values. This shows that the current tracking is well tuned in the low frequency ranges. Also, this controller should not affect from $G_e(p)$ in current regulation system as an input disturbance. Fig. (4) shows the tracking error $(|G_e(j\omega))$ in percentage values. As depicted in Fig. (4), eliminating steady-state error and reducing the back-EMF influences in closed-loop system is possible. In order to evaluate the sensitivity of the desired controller to the transient inductance of the induction machines, changes have been made in the value of this inductance. Also, the current tracking is done without sensitivity to this parameter in the low frequency ranges.

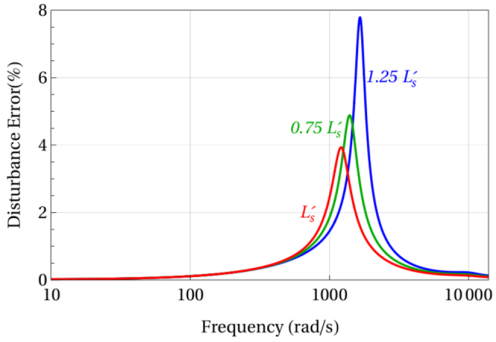

Fig.4. Frequency response of the proposed current regulator in the SRF for disturbance tracking error in percentage with different transient inductances.

6. NUMERICAL AND EXPERIMENTAL RESULTS

Fig. (5) illustrates performances of the proposed current controller without back-EMF signals at the ω_r=45 rad/sec. The tracking errors of the stator currents between fundamental component and reference currents have been depicted. In this result, the current amplitudes of the direct and quadrature components of the stator reference currents have decreased from 0.5 A to 0.35 A at t=0.5 seconds. Also, the frequency of the reference currents decreases from 20 rad/sec to 15 rad/sec at t=0.25 seconds. These results show that the current tracking errors with fast dynamics follow their reference values. Therefore, without using the decoupling signals, by choosing a PI controller instead of a PR controller, it is possible to get the desired responses of the drivers.

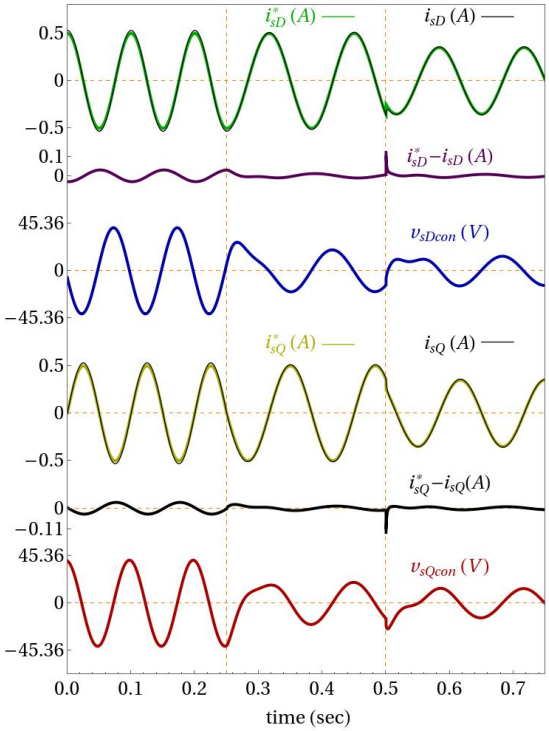

Fig.5 Transient perfomaces of the proposed current controller in SRF with averaged model of the VSI.

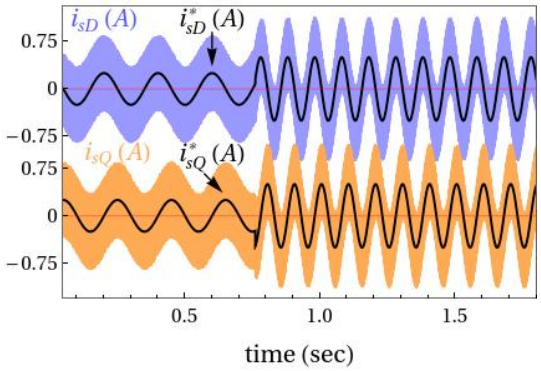

Fig. 6. Switching performances of the proposed current controller in the SRF.

Another performance of the current controller in an induction driver is the effects of driver disturbances and inverter switching in current tracking. For this purpose, in the simulation presented in Fig. (6), the switching model of the inverter without using voltage decoupling circuit in the SRF is considered. In this condition, the amplitude and frequency of the stator current increases from 0.25 A with 5 Hz to 0.5 A with 10 Hz at t=0.75 seconds. The modulation method of inverter is also applied by PWM technique. The more details of the switching signal along with the control voltage of the PWM modulator and i_{sD} around the t=0.75 seconds are shown in Fig. (7). These results depict that despite

the ripple of the large ratio of the stator current; the current tracking is well done with fast transient response.

In order to practical evaluate the proposed controller; experimental tests are conducted to verify the effectiveness of the current controller. The test bench for implementing this system is shown in Fig. (8). This laboratory setup consists of a two-phase IM, a VSI with insulated gate bipolar transistor (IGBT), and a personal computer. A personal computer with Windows operating system has long lags and interruptions. To achieve high sampling rate in the practical implementation, the Linux operating system is considered.

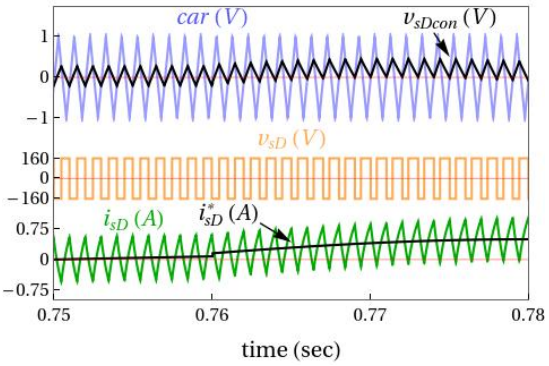

Fig.7. Direct current control signals of the proposed current controller in the SRF.

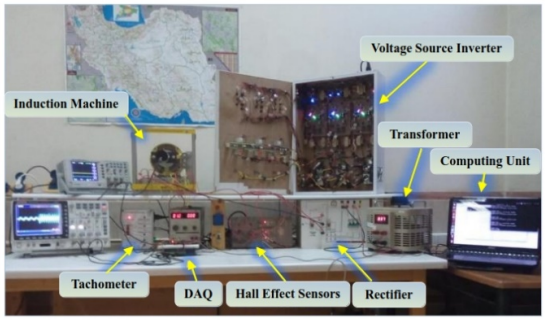

Fig.8. Test bench of the proposed current controller in the SRF.

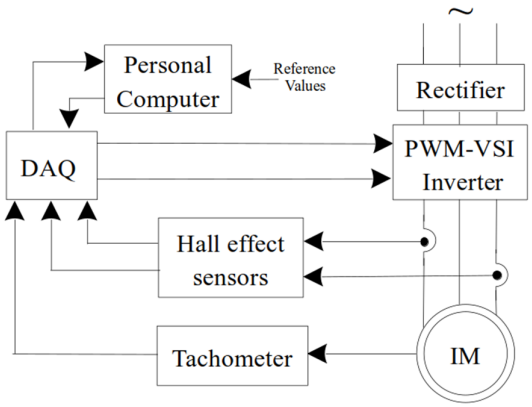

Fig.9. Block diagram of the closed-loop system.

Also, Advantech DAQ USB4711-a is used to read the speed encoder signals and two hall effect current sensors. Moreover, DAQ create the switching command signals of the VSI. The parameters of this system are extracted from Table 1. Fig. (9) shows the experimental result for direct and quadrature of the stator currents.

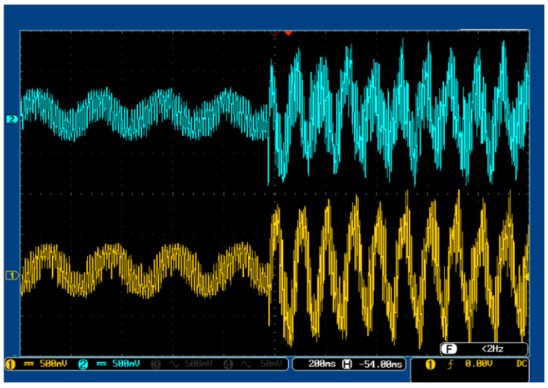

Fig.10. Experimental results of the proposed current controller in the SRF.

Fig. (7) in comparison to Fig. (10) shows, the experimental measurements have confirmed the numerical results with zero steady-state tracking error and a fast transient response for the closed-loop system in the SRF.

7. CONCLUSION

A well-known PI current regulator in the SRF is virtually accepted as suffering from steady-state error. In this paper, a methodology for designing a current controller to track the reference current in the SRF with near zero steady-state error was presented. As a result, the reference currents can be tracked by the proposed controller without any back EMF signals and decoupling circuits. Therefore, the compilation process is reduced in the closed-loop system and also, the system relies less on the speed measurement than the conventional system in the SRF due to the elimination of the feed-forward correction signals.

REFERENCES

[1] T. A. Lipo, Vector control and dynamics of AC drives, vol. 41. Oxford university press, 1996.
[2] P. Vas, Sensorless vector and direct torque control. Oxford Univ. Press, 1998.
[3] I. Boldea and S. A. Nasar, Vector control of AC drives. CRC press, 1992.
[4] N. R. N. Idris, C. L. Toh, and M. E. Elbuluk, "A new torque and flux controller for direct torque control of induction machines," Industry Applications, IEEE Transactions on, vol. 42, no. 6, pp. 1358–1366, 2006.
[5] D. Casadei, F. Profumo, G. Serra, and A. Tani, "FOC and DTC: two viable schemes for induction motors torque control," Power electronics, IEEE Transactions on, vol. 17, no. 5, pp. 779–787, 2002.

[6] D. Casadei, G. Serra, A. Stefani, A. Tani, and L. Zarri, "DTC drives for wide speed range applications using a robust flux-weakening algorithm," Industrial Electronics, IEEE Transactions on, vol. 54, no. 5, pp. 2451–2461, 2007.
[7] L. Zarri, M. Mengoni, A. Tani, G. Serra, D. Casadei, and J. Ojo, "Control schemes for field weakening of induction machines: A review," in Electrical Machines Design, Control and Diagnosis (WEMDCD), 2015 IEEE Workshop on, pp. 146–155, IEEE, 2015.
[8] A. Trzynadlowski, The field orientation principle in control of induction motors, Springer Science & Business Media, 2013.
[9] D. G. Holmes, B. P. McGrath, and S. G. Parker, "Current regulation strategies for vector-controlled induction motor drives," Industrial Electronics, IEEE Transactions on, vol. 59, no. 10, pp. 3680–3689, 2012.
[10] T. H. Nguyen, T. L. Van, D.-C. Lee, J.-H. Park, and J.H. Hwang, "Control mode switching of induction machine drives between vector control and v/f control in over modulation range," Journal of Power Electronics, vol. 11, no. 6, pp. 846–855, 2011.
[11] R. A. Sangrody, J. Nazarzadeh, and K. Y. Nikravesh, "Inherent chaotic behavior in vector control drives of induction machines," Electric Power Components and Systems, vol. 40, no. 1, pp. 1–20, 2011.
[12] S. H. Hamdy Mohamed Soliman, "Improved hysteresis current controller to drive permanent magnet synchronous motors through the field-oriented control," International Journal of Soft Computing and Engineering (IJSCE), vol. 12, no. 4, pp. 40–46, 2012.
[13] D. G. Holmes, R. Davoodnezhad, and B. P. McGrath, "An improved three-phase variable-band hysteresis current regulator," Power Electronics, IEEE Transactions on, vol. 28, no. 1, pp. 441–450, 2013.
[14] Y.-H. Choi, N.-S. Cho, W.-H. Kwon, and D.-H. Lee, "Design of switching frequency limiter for hysteresis current controlled PWM vsi," in Control, Automation and Systems (ICCAS), 2013 13th International Conference on, pp. 431–433, 2013.
[15] H. Akbari, and J. Nazarzadeh. "Stabilizing and Control of the DC-Microgrid Systems with PV Panels and CPLs." Electrica, vol. 24, no. 1, pp. 39-50, 2024.
[16] Abdol M, Nazarzadeh J. "A Comparison Study between Different Decoupling Circuits & Inverter Models in Induction Drives for FOC", 3rd International Conference on Electrical Machines and Drives (ICEMD) 2023 Dec 20, pp. 1-7, 2023.
[17] M. H. Holakooie, A. Taheri, and M. B. B. Shari-fian, "Mras based speed estimator for sensorless vector control of a linear induction motor with improved adaptation mechanisms," Journal of Power Electronics, vol. 15, no. 5, pp. 1274–1285, 2015.
[18] D. Holmes, T. Lipo, B. McGrath, and W. Kong, "Optimized design of stationary frame three phase ac current regulators," Power Electronics, IEEE Transactions on, vol. 24, no. 11, pp. 2417–2426, 2009.
[19] D. N. Zmood and D. G. Holmes, "Stationary frame current regulation of PWM inverters with zero steady-state error," Power Electronics, IEEE Transactions on, vol. 18, no. 3, pp. 814–822, 2003.
[20] D. N. Zmood, D. G. Holmes, and G. H. Bode, "Frequency-domain analysis of three-phase linear current regulators," Industry Applications, IEEE Transactions on, vol. 37, no. 2, pp. 601–610, 2001.